

NASA Technical Memorandum 104088

10304
P12

**TRANSONIC SHOCK-INDUCED DYNAMICS OF A FLEXIBLE WING
WITH A THICK CIRCULAR-ARC AIRFOIL**

**ROBERT M. BENNETT
BRYAN E. DANSBERRY
MOSES G. FARMER
CLINTON V. ECKSTROM
DAVID A. SEIDEL
JOSÉ A. RIVERA, JR.**

(NASA-TM-104088) TRANSONIC SHOCK-INDUCED
DYNAMICS OF A FLEXIBLE WING WITH A THICK
CIRCULAR-ARC AIRFOIL (NASA) 12 6 CSCL 01A

N91-27132

Unclass

03/02 0024604

MAY 1991



National Aeronautics and
Space Administration

Langley Research Center
Hampton, Virginia 23665



TRANSONIC SHOCK-INDUCED DYNAMICS OF A FLEXIBLE WING WITH A THICK CIRCULAR-ARC AIRFOIL

Robert M. Bennett*, Bryan E. Dansberry†, Moses G. Farmer‡, Clinton V. Eckstrom§,
David A. Seidel¶, and José A. Rivera, Jr.‡

NASA Langley Research Center
Hampton, VA 23665-5225

Abstract

Transonic shock-boundary layer oscillations occur on rigid models over a small range of Mach numbers on thick circular-arc airfoils. Extensive tests and analyses of this phenomena have been made in the past but essentially all of them were for rigid models. A simple flexible wing model with an 18% circular arc airfoil was constructed and tested in the Langley Transonic Dynamics Tunnel to investigate the dynamic characteristics that a wing might have under these conditions. In the region of shock-boundary layer oscillations, buffeting of the first bending mode was obtained. This mode was well separated in frequency from the shock boundary layer oscillations. A limit cycle oscillation was also measured in a "third bending-like" mode, involving wing vertical bending and splitter plate motion, which was in the frequency range of the shock-boundary layer oscillations. Several model configurations were tested, and a few potential fixes were investigated.

Nomenclature

BM	model wing root bending moment
c	wing chord
k	reduced frequency based on semichord, $\omega c/2V$
q	dynamic pressure
RMS	root-mean-square value
S	wing area
V	freestream velocity
ω	frequency of oscillation, rad./sec

Introduction

The transonic speed range can be particularly troublesome for aircraft. Minimum flutter speed, buffeting, nonclassical flutter modes, limit cycle oscillations, and control surface buzz are among the potential aeroelastic problems. These phenomena are

*Sr. Aerospace Engineer, Unsteady Aerodynamics Branch, Associate Fellow AIAA

†Aerospace Engineer, Configuration Aeroelasticity Branch

‡Aerospace Engineer, Configuration Aeroelasticity Branch, Member AIAA

¶Aerospace Engineer, Unsteady Aerodynamics Branch, Member AIAA

§Asst. Head, Configuration Aeroelasticity Branch, Member AIAA

particularly difficult to analyze as the unsteady flows involve moving shock waves and significant viscous effects coupled with the structural dynamics of the aircraft. The unsteady transonic aerodynamic problems have recently been summarized in reference 1.

There are some transonic flows that are naturally oscillatory even when the boundary conditions are steady. A notable example is the transonic shock-boundary layer oscillations that occur on thick rigid circular-arc airfoils over a small range of Mach numbers. This shock-boundary layer oscillation problem has been extensively studied (see, for example, ref. 2-15). The conditions for this oscillation are illustrated in figure 1. As Mach number is increased subsonically, the strength of the shocks terminating the supersonic region on the fore part of the airfoil increases. Initially, a small separation zone occurs at the foot of the shock and at the trailing edge. As the Mach number is further increased, the flow over the airfoil becomes fully separated behind the shock wave. On the thick circular-arc airfoils, near the Mach numbers where the transition from partial to fully separated flows takes place, there is a Mach number range of about 0.04 where the flow alternates antisymmetrically from partially attached to fully separated flow. This occurs with large pressure changes yielding an alternating lift coefficient of about 0.10 at a high frequency, which for the 18% thick airfoil is at a reduced frequency ($k = \omega c/2V$) of about 0.50. Much of the understanding of this flow has come from flow visualization and unsteady pressure measurements (ref. 2, 3, 7, and 9), but some success has also been achieved in calculating this phenomena (see ref. 1, Chap 5, and ref. 5).

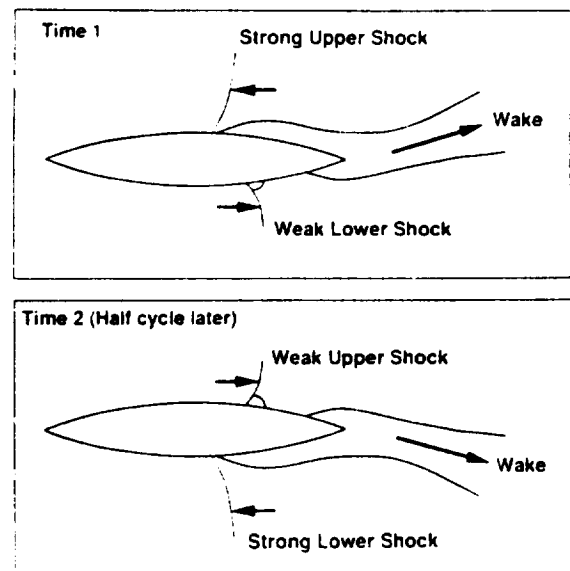


Figure 1. Sketch of transonic shock-boundary layer oscillation on circular-arc airfoil.

Although the studies on the circular arc airfoil are more extensive, transonic shock oscillations on other airfoils such as the NACA 0012^{16,17} and supercritical airfoils¹⁷⁻²⁰ have been identified in other studies. Many of these oscillation cases occur at nonzero angles of attack and with shocks on one side of the airfoil only. The reduced frequency for the oscillations can be as low as 0.25 which is of the order of half those for the thick circular arc airfoil.¹⁶ Some success has also been achieved in calculating such flows.^{17,18}

For the thick circular-arc airfoils, several investigators have examined devices such as holes through the airfoil^{11,14}, spanwise wires¹¹, altered trailing edges^{11,14}, and porous sections¹³ around the shock location, as a mean of eliminating or suppressing the shock boundary layer oscillations. Many of these devices or fixes have been quite successful.

With the exception of reference 10, which considered some low frequency torsional oscillations, the extensive investigations of this phenomena for the circular arc airfoil, both test and analysis, have been for rigid models. To examine the aeroelastic behavior of a wing with such aerodynamic oscillations, a simple flexible rectangular wing model with an 18% circular-arc airfoil was constructed. The wing model was tested in the Langley Transonic Dynamics Tunnel. The effects of several configuration variables were investigated including reduced stiffness, transition strip, splitter plate, spanwise strip, vortex generators, and reduced span. This paper describes the model, the wind tunnel tests, and presents a summary of the measured results.

The model was instrumented with strain gages and accelerometers and no unsteady pressure measurements were made. The shock-boundary layer oscillation frequencies are available from the literature and have been shown to occur on finite-span wings of similar aspect ratio.⁹ The existence and frequency of the shock-boundary oscillation for the tests of the simple model described herein are thus inferred from measurements of the dynamic response of the model.

This project is a part of the Benchmark Models Program of the Structural Dynamics Division of the NASA Langley Research Center. The Benchmark Models Program is a multi-year program that primarily focuses on providing data for Computational Fluid Dynamics (CFD) code calibration. Additional goals are to increase the understanding of unsteady flows, and to provide empirical data for design purposes. This investigation with a simple model is aimed at increased understanding of transonic aeroelastic phenomena rather than CFD code calibration.

Test Apparatus and Procedures

Wind Tunnel

The wind tunnel tests were conducted in the Langley Transonic Dynamics Tunnel (TDT). The TDT is a slotted-throat, variable pressure, single-return wind tunnel having a test section 16 feet square (with cropped corners). It is capable of operation at Mach numbers up to 1.2 and at stagnation pressures from near vacuum to atmospheric. The tunnel is equipped with four quick-opening bypass valves which can be used to rapidly reduce test-section dynamic pressure and Mach number when flutter occurs. Although either air or a heavy gas can be used as a test medium, only air was used for the present tests.

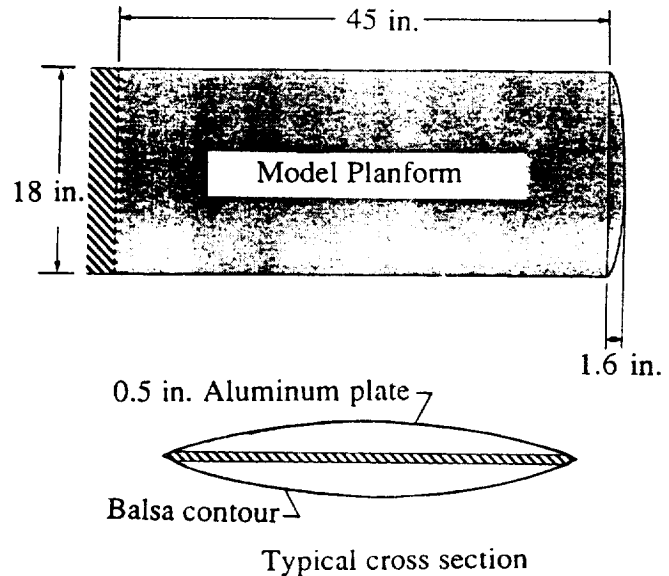


Figure 2. Sketch of wing model.

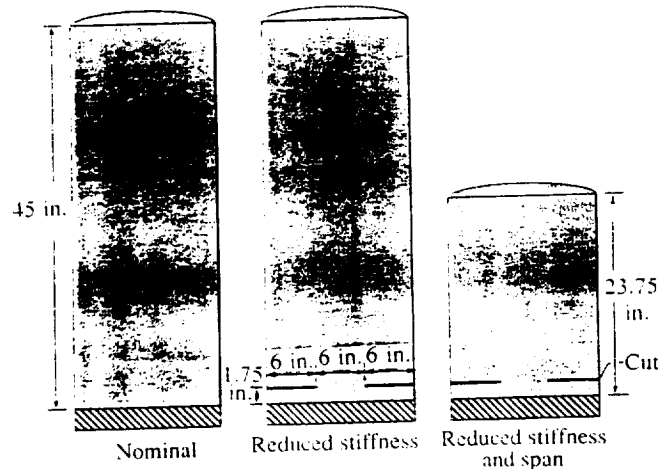


Figure 3. Sketch of configurations tested.



Figure 4. Wing with 18% circular arc airfoil mounted in the Transonic Dynamics Tunnel

Model

A sketch of the semispan model tested is given in figure 2. The model was rectangular in planform, 18 inch chord by 45 inch span, and was of simple construction. The central portion was a 0.50 inch aluminum flat plate with edges machined to form a bevel. Balsa was glued to the plate with the grain running spanwise and formed to an 18 percent circular-arc airfoil section with sharp leading and trailing edges. A balsa wood tip of revolution was added. A 0.50 inch wide transition strip of no. 30 grit was added beginning at ten percent chord. Using this method of construction, the model was somewhat stiffer and heavier than might be expected from a typical scaled aircraft aeroelastic model. Since the model was inexpensive and of relatively simple construction, significant modifications could be made conveniently in the tunnel during the test. The wing stiffness was reduced to lower the frequencies by sawing the plate one quarter-chord in from both the leading and trailing edges (see figure 3). Later in the test the span was reduced by sawing off the outer part of the wing and reattaching the tip of revolution (fig. 3). Although the model was reasonably well constructed, the surface finish was not entirely smooth apparently as a result of local contraction and expansion of the balsa wood.

The root of the plate of the model was clamped in a near cantilever fashion to a remotely operable turntable so that the angle of attack could be set. A splitter plate of about 6 feet in length and 3 feet high was used to keep the root of the model outside the tunnel wall boundary layer. The model is shown mounted in the TDT in figure 4.

The splitter plate was made from an aluminum sheet with L-shaped doublers on the back side. It was attached to the mounting bracket clamping the wing to the turntable. Four braces also extended from the inboard portion of the mounting bracket to the outer four corners of the splitter plate. Such an arrangement facilitated angle of attack change of the model as the splitter plate would pitch with the model. The splitter plate, however, acted much like a panel in vibration and participated in motion of the higher vibration modes of the wing. The model frequencies for the configuration tests are given in Table I. The mode near 90 Hz is a "third-bending-like mode" that also involves splitter plate motion. The frequency of this "third-bending-like mode" is much lower than one would anticipate for a cantilever wing, apparently as a result of coupling with the splitter plate motion. The model frequencies without the splitter plate were more nearly those one would expect for a cantilever wing. There were also two torsion modes that differed in frequency and splitter plate motion (Table 1).

Tests

Two tunnel entries were conducted. The first was a brief exploratory test of two runs to assess the character of the response. The first run was with the complete wing as fabricated. The wing root was then cut to reduce stiffness (fig. 2) and another run was made. Later, a second tunnel entry was made to explore several configuration variables over several runs. The model was cut to reduce the aspect ratio near the end of the second entry.

The model was tested by varying Mach number in small increments at a nearly constant tunnel pressure. For some configurations only one or two total pressures were used to examine the measured trends. For the cut configuration several variations in total pressure were made to examine trends over a wide range of dynamic pressure. Angle of attack was maintained to be near zero by observing root strain and keeping it near zero by varying the turntable angle. The Reynolds number for these tests generally ranged from about 1.0×10^6 to 1.8×10^6 based on the model chord.

Instrumentation and data processing

The model was instrumented with four accelerometers and two strain gages. The strain gages were mounted on the wing plate near the root to measure bending and torsional moments. The accelerometers were mounted at 14% and 86% of chord at 50% and 96% of the original span. Only the inboard two accelerometers were retained for the reduced span configuration. During the test the model response was viewed visually through the control room window, and the instrument output was monitored on a strip chart recorder and with a spectral analyzer. The tunnel conditions, and the strain gage and accelerometer output were also recorded on digital tape. Twenty seconds of data in engineering units were recorded by the tunnel data system at 1000 samples/second to be used for additional data analysis.

For some portions of the test, shear-sensitive liquid crystals²¹ were sprayed on the wing and the resultant patterns observed during testing were recorded with a color video camera. These crystals change color with surface shear and, for cases of strong shocks, can be used in the spirit of oil flows to give some indication of shock location along the wing.

Time histories of the digitized data were plotted and the means, maxima and minima, and power spectra were computed for summary plots. Most of the response of the bending gage was in the 1st bending mode and in the mode near 90 Hz. The data were then digitally filtered with a low pass filter (below about 25 Hz) and a high pass filter (above about 25 Hz) to determine the individual modal

Table 1. MEASURED FREQUENCIES

Mode	Basic Model	Cut at Root	Without Splitter Plate	Shortened Span
1st Bending	11 Hz	7.8 Hz	7.6 HZ	20 Hz
Total	51 Hz 59 Hz	43 Hz 44 Hz	44 Hz	79 Hz
2nd Bending	70 Hz	68 Hz	70 Hz	
3rd Bending-splitter plate	94 Hz	92 Hz		

Results and Discussion

contributions to the RMS response. The low-pass filtered signal essentially contains only the response of first bending mode and the high-pass filtered signal generally contains only the response of the "third-bending-like" mode or the shock-boundary layer oscillations.

All the data presented herein are from the bending strain gage. No results are presented for the full span nominal configuration or the reduced span wing although both are briefly discussed.

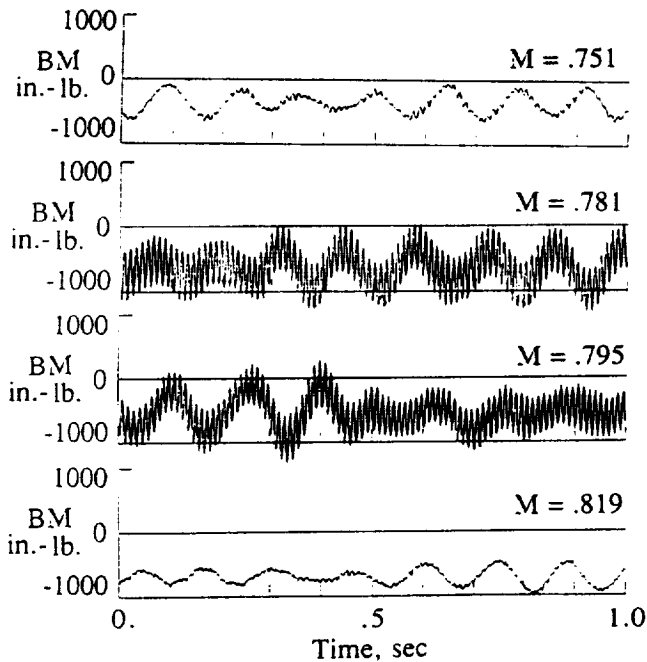


Figure 5. Sample of time histories of bending moment response.

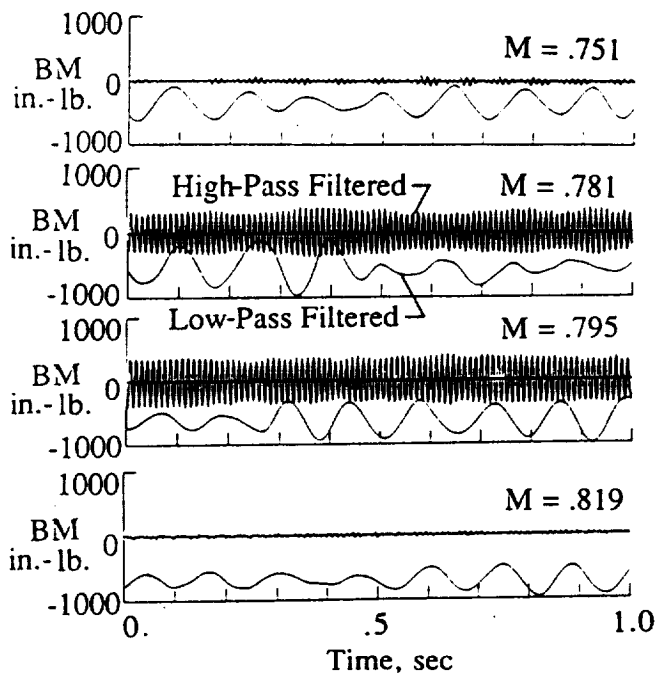
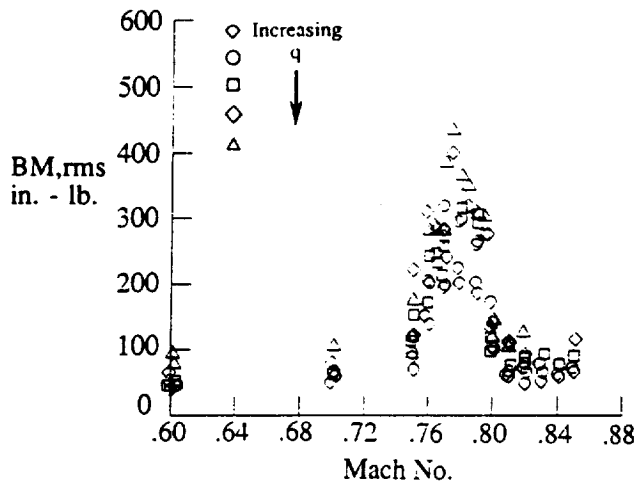


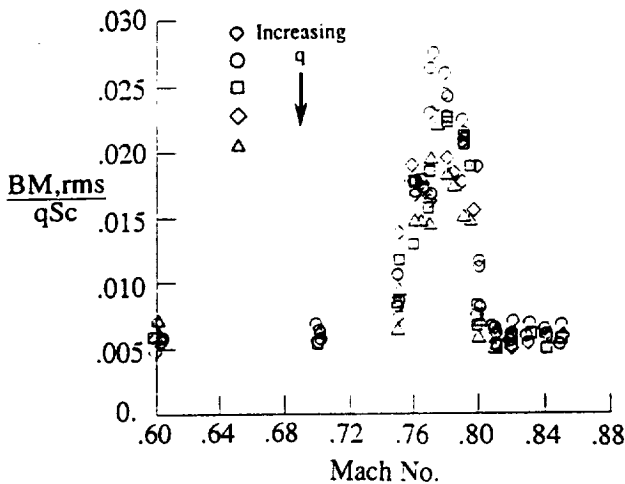
Figure 6. Sample of low and high-pass filtered time histories

Character of Measured Results

The overall character of the results is illustrated in the short segment of time histories presented in fig. 5. For low Mach numbers, the first bending mode responded at its frequency with random beating or bursts of motion typical of a buffeting response (fig. 5, M = 0.751). As Mach number was increased, the buffeting of the 1st bending mode increased and a nearly constant amplitude response in the 3rd bending mode was also observed (fig. 5, M = 0.781). Further small increases in Mach number resulted in little change (fig. 5, M = 0.795), until slightly above a Mach number of 0.80 no further response of the 3rd bending mode was apparent (fig. 5, M = 0.819). Bending response was obtained only in the 1st and 3rd bending mode and not in the 2nd bending mode.



a. Total response



b. Nondimensional total response

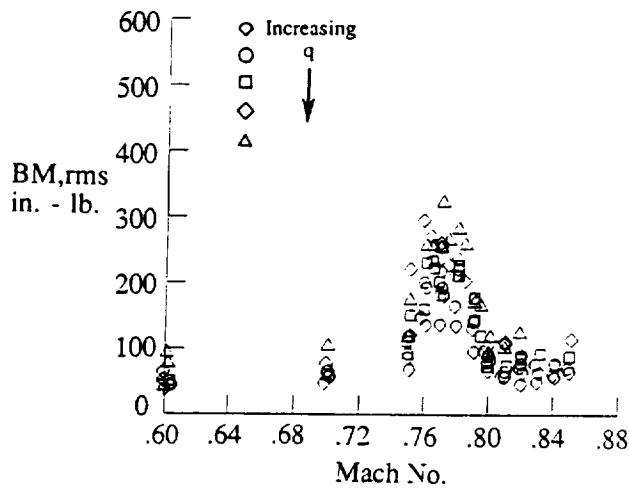
Figure 7. Bending moment response measurements for several wind tunnel pressures. Reduced stiffness wing.

The response of the bending modes can be seen more clearly in the filtered time histories of fig. 6. The signal was passed through low and high pass digital filters and the response plotted. The high frequency (3rd bending) is clearly seen to be limit-cycle or constant-amplitude response.

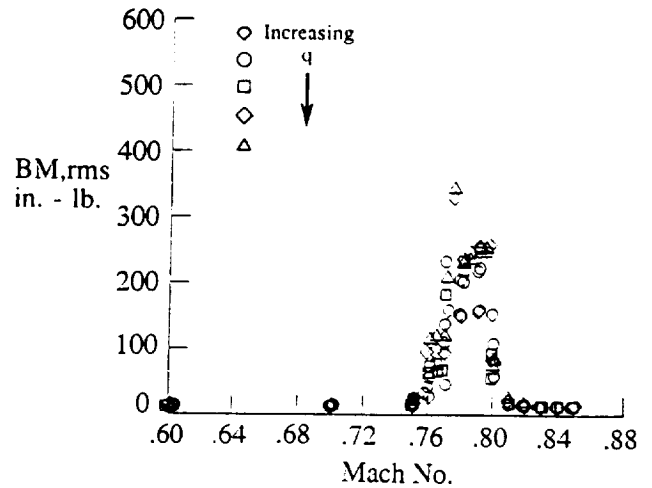
The total (broad band) root-mean-square (RMS) response of the root bending moment measurement is presented in fig 7a in physical units and in the form of bending moment coefficient (bending moment divided by dynamic pressure x area x chord) in fig. 7b. The bending moment response increases rapidly near $M = 0.76$ and decreases rapidly again near $M = 0.80$. This corresponds closely to the Mach number range of the shock-boundary layer oscillation for the 18% circular arc airfoil (ref. 6). The response increases with dynamic pressure, but normalizing by dynamic pressure only slightly improves the correlation. For these data, dynamic pressure was varied from about 50-130 psf at $M = 0.60$, from about 85-200 psf at $M = 0.78$, and from 90-210 psf at $M = 0.82$.

Similar root-mean-square (RMS) responses were calculated after low-pass and high-pass filtering and are presented in dimensional form in figs. 7c and 7d. The peak RMS responses in both modes are about equal. The correlation of the response of the first mode is again only slightly improved by dividing by dynamic pressure (fig. 7e) although there is generally more response in the 1st mode at the higher dynamic pressure than at the low dynamic pressure (fig. 7e). The high frequency results tend to be limited (fig 7d) even though dynamic pressure is increased (with exception of the two points at $M = 0.77$). This is further indicated by the nondimensional results of figure 7f.

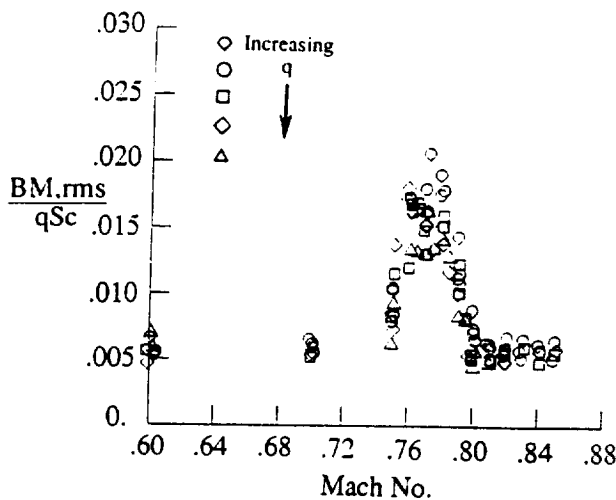
These results further indicate that the region of shock-boundary layer oscillations led to a buffeting condition on this wing for the 1st bending mode which was well removed in frequency from the aerodynamic oscillations, and also that the oscillation encountered in the 3rd bending-like mode was a limit-cycle oscillation. From the literature^{6,7} the reduced frequency of the shock-boundary layer oscillations is approximately $k = 0.50$. Dimensional frequency based on



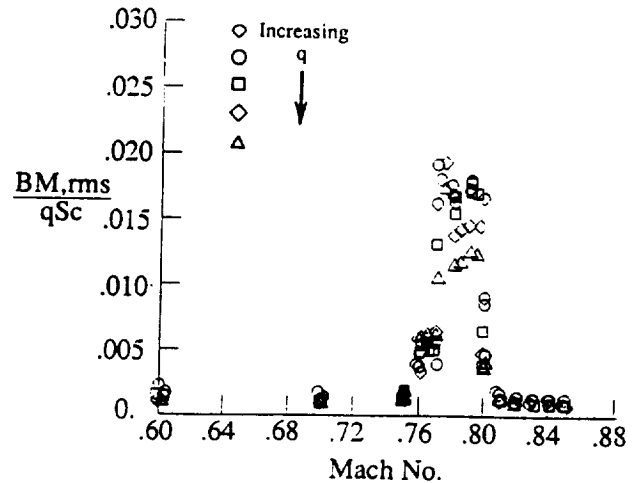
c. Filtered low frequency response



d. Filtered high frequency response



e. Filtered nondimensional low frequency response



f. Filtered nondimensional high frequency response

Figure 7. Concluded

this k-value is calculated to be 93 Hz, which is quite near the 3rd bending-like modal frequency.

The sequence of approach to the limit cycle oscillation is also demonstrated by the power spectra of bending moment presented in figure 8. The oscillation initially arises near $M = 0.76$ and near 80 Hz. As Mach number is increased, the frequency of oscillation increases and appears to lock in for the limit cycle oscillation. At higher Mach numbers the model response diminishes. Either the shock boundary layer oscillation frequency is significantly above the model frequency, or the shock boundary layer oscillation ceases as the boundary layer stabilizes in a fully shock-induced separated state.

The character of the results for the uncut configuration of the first entry were similar to those presented in figure 5, but with reduced amplitude of the buffeting of the first mode. No data for the uncut configuration are presented.

A liquid crystal pattern for $M = 0.82$ is shown in figure 9. At this Mach number the flow behind the shock should be non-oscillatory and fully separated. The light line gives an indication of the shock location and shows a nearly constant chord location over much of the span. However a strong tip effect with a complex flow pattern is evident.

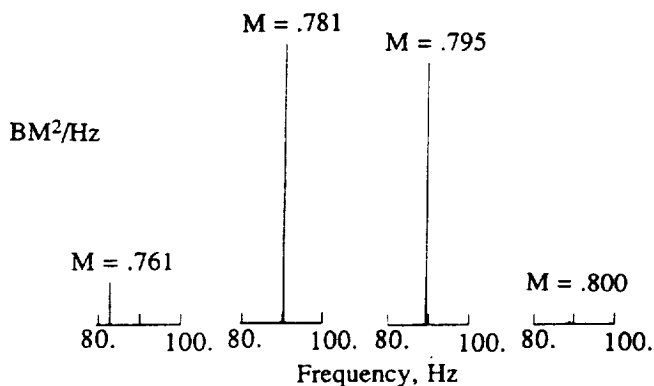


Figure 8. Portion of power spectra of bending moment for several Mach numbers.

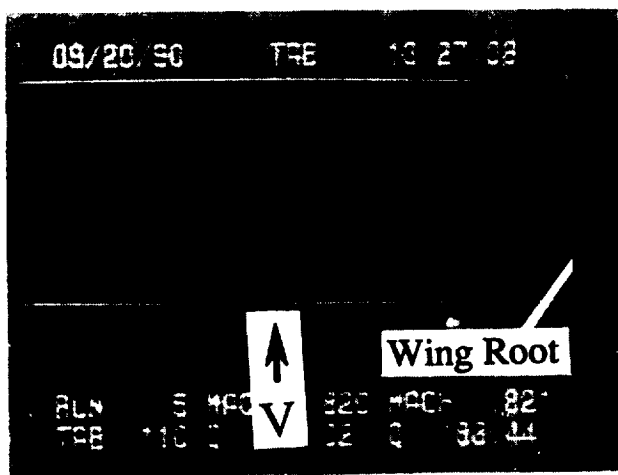


Figure 9. Liquid crystal pattern on wing, $M = 0.82$.

Test without the Splitter Plate

As previously discussed, "the third bending like" mode involved coupled splitter plate motion. The splitter plate was removed for one run. The portion of the model inboard of the splitter plate location was not aerodynamically faired and had sharp edges. The model frequencies are given in Table I. Second bending at 70 Hz is the only frequency found on the wing in the 70-140 Hz range. The low-and high-pass filtered results are shown in figure 10. The buffeting response in the first bending mode is near the same level as with the splitter plate (fig. 7c). However the variation in the RMS response with Mach number for the higher frequency range is similar to that obtained previously (fig. 7f) but at a significantly reduced level. This would appear to be forced response driven by the aerodynamic oscillations, whereas the higher response observed with the splitter plate involves a coupled response of the aerodynamic oscillations and the "3rd bending-like" mode.

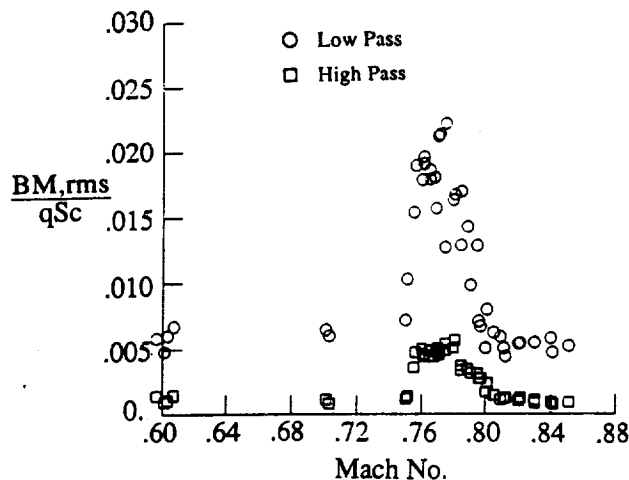


Figure 10. Filtered bending moment response measured without splitter plate.

Effect of Free Transition

It has been shown (ref. 7) that for 14% thick circular-arc airfoils, transonic shock boundary oscillations exist for low Reynolds number laminar flows and for high Reynolds number turbulent flows, but may disappear for transitional flows. One run was made without a transition strip to examine the effect of the transition strip. The low-and high-pass-filtered bending moment results are shown in figure 11. The high frequency results indicated that the aerodynamic oscillations nearly disappeared. The low frequency results, however, are significantly larger than for the results with the transition strip. (Note the change in scale from the previous figures.) In fact, a large amplitude flutter condition with a frequency near the 1st bending frequency, was encountered near $M = 0.75$. This occurred as Mach number was being decreased from $M = 0.85$ and at nearly the same conditions that had been traversed going to $M = 0.85$. Flutter resulting from the transition point varying during a cycle of motion has been discussed by Mabey²². The present results indicate that the transition free results can be erratic in this Reynolds number range ($1.0-1.8 \times 10^6$) and obtaining consistent results requires fixed transition.

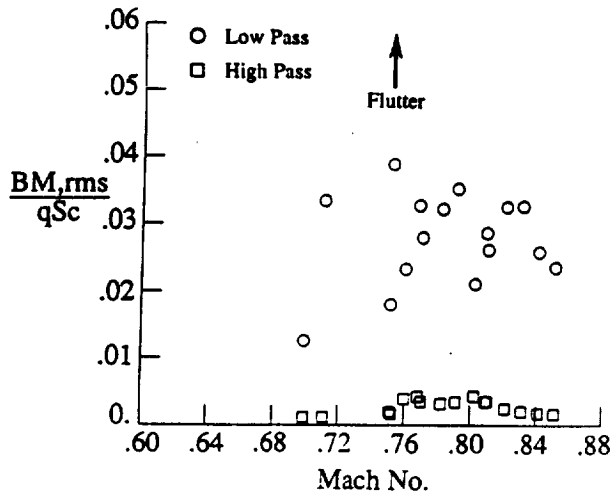
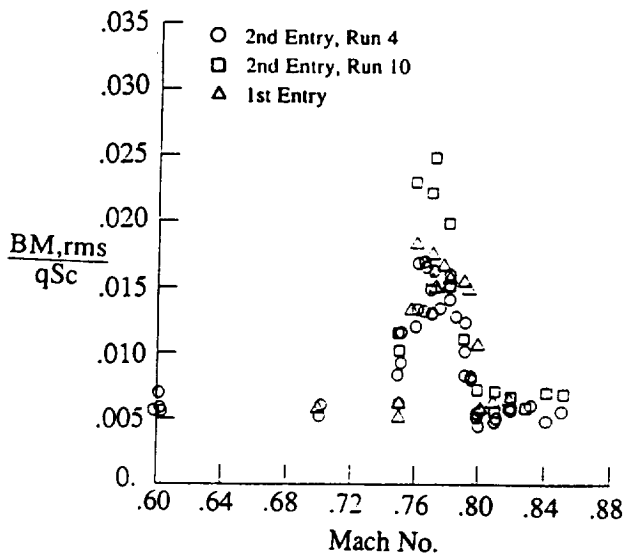
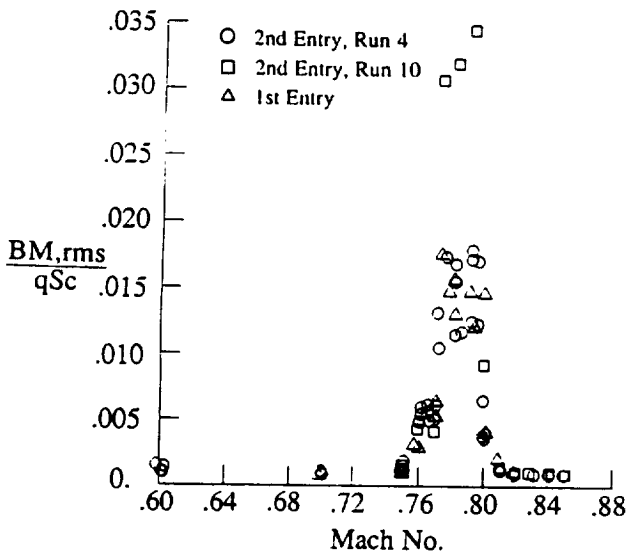


Figure 11. Filtered bending moment response measured with free transition.



a. Low frequency response



b. High frequency response

Figure 12. Comparison of measured results for same configuration.

Repeatability

Similar runs were made for both wind tunnel entries and again later in the second entry. These results are summarized in figures 12a and 12b. The results for the first entry and for run 4 of the second entry compare remarkably well for this type of data. However, the high frequency response for run 10 of the second entry are somewhat larger than for the others. The reason for this is not clear, but could be related to differences in the details of the transition strip or model fatigue.

Effect of Spanwise Strip

A spanwise wire located aft of the shock wave was shown to be a good fix or suppressor of the shock-boundary layer oscillations in ref. 11. In the present study, a 0.25 inch square strip with rounded corners was taped to the surface at $x/c = 0.75$ on both upper and lower surfaces. This strip extended from 1 inch inboard of the tip to 2 inches outboard of the splitter plate. This type of fix is essentially a verification of the understanding of this phenomena as it basically interrupts the alternating separation and reattachment. The low and high frequency results are shown in figure 13. The high frequency oscillations are effectively suppressed. However the trend for the low frequency buffeting shown (fig. 13) persisted at lower Mach numbers and a large increase in buffeting levels was obtained. A data point (not shown in fig. 13) at $M = 0.43$ gave a bending moment coefficient of 0.033 which is a pronounced increase in buffeting level. In summary, the spanwise strip eliminates the high frequency oscillation but has the strong and undesirable side effect of increased subsonic buffeting response.

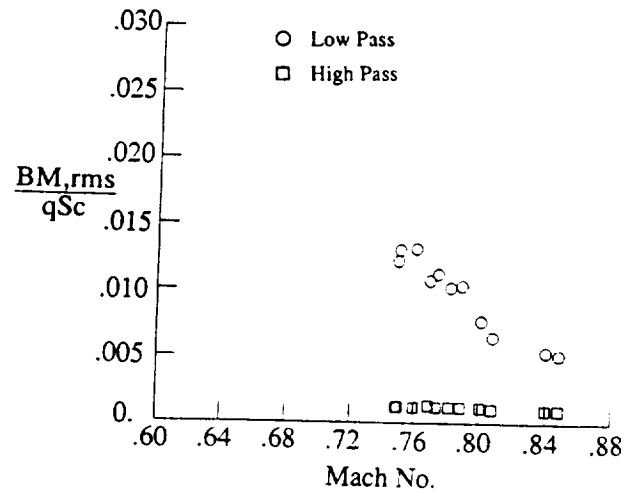


Figure 13. Filtered measured bending moment with spanwise strip.

Effect of Vortex Generators

Several types of vortex generators have been used for some time to alleviate shock-boundary layer interactions. One type that has been applied is the Wheeler wishbone-type of vortex generators. These are generally used as sub-boundary layer devices and are effective at a height of 0.2 to 0.3 of the boundary layer thickness for turbulent boundary layers. Consequently they have lower drag than devices that extend outside the boundary layer. These sub-boundary layer devices have been used for alleviation of an unsteady shock boundary layer oscillation on a fuselage canopy,²³ and for separation control.²⁴⁻²⁵ For this test, they were applied to the circular arc model as shown on the model in figure 14. A mix of 0.100-inch and .096-inch high generators were applied from 3 inches inboard of the tip to 3 inches outboard of the root at 60% chord for the first configuration. These generators were higher than would be considered sub-boundary layer devices for the model. The low and high frequency test results are shown in figure 15. The high frequency oscillations were effectively suppressed, but the low frequency buffeting grew in the transonic range. A large flutter-like response, with a frequency near the 1st bending frequency, was encountered near $M = 0.80$ (fig. 15).

The vortex generators were moved to 45% chord and extended from 3 inches inboard of the tip to 15 inches outboard of the root as the second configuration. (Some of the inboard vortex generators were lost in an earlier run.) The results shown in figure 16 indicate some reduction in the low frequency of buffeting but little effectiveness for the high frequency mode at this forward location. This type of vortex generator, as well as the other types, may have potential for alleviating this type of shock-boundary layer interaction but must be carefully designed and require further development. The use of small wind tunnels and rigid models for such an effort is appropriate, but the present tests suggests that the results need to be checked for side-effects such as increased buffeting or flutter on a dynamic model.

Effects of Shortened Span

The span of the wing was reduced in an effort to raise the model torsional frequency up into the range of the shock-boundary layer oscillation frequency. The reduction in span gave a torsion frequency of 79 Hz. (Table 1). Spectral analyses of the root torsional moment (not shown) indicated a sharp peak that passed through the torsional frequency as Mach number was increased. However, although the root torsional moments increased significantly (RMS-levels), the time history of the responses were of a beating nature and did not lock into a constant-amplitude limit-cycle oscillation as was the case for the high frequency bending mode of the longer wing. Sustained torsional oscillations have been obtained for a swept wing at transonic separated-flow conditions.²⁶

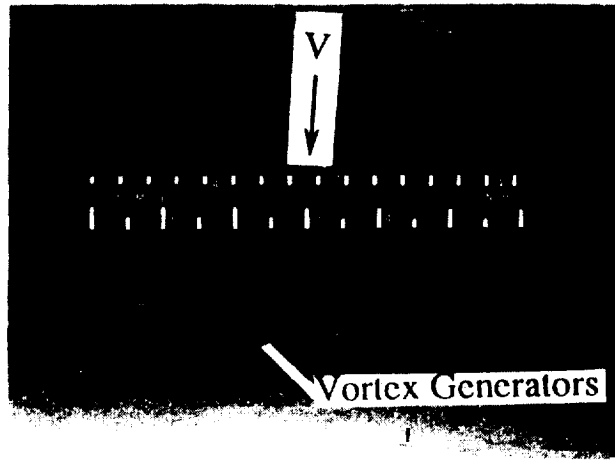


Figure 14. Photograph of wing with vortex generators, configuration 1.

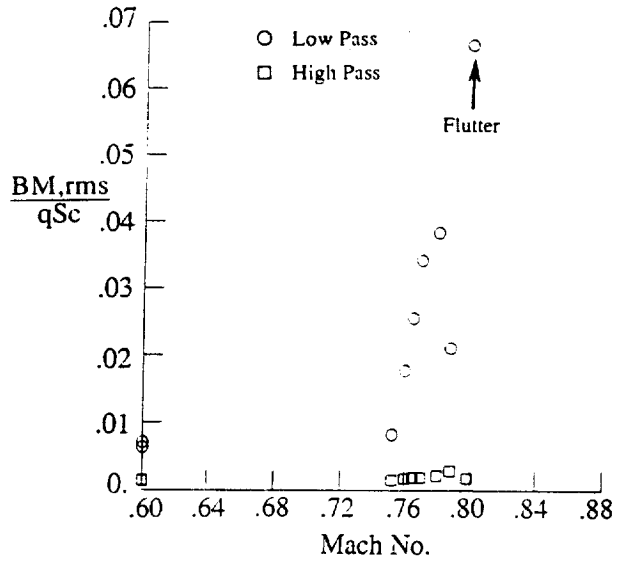


Figure 15. Filtered measured bending moment with vortex generators, configuration 1.

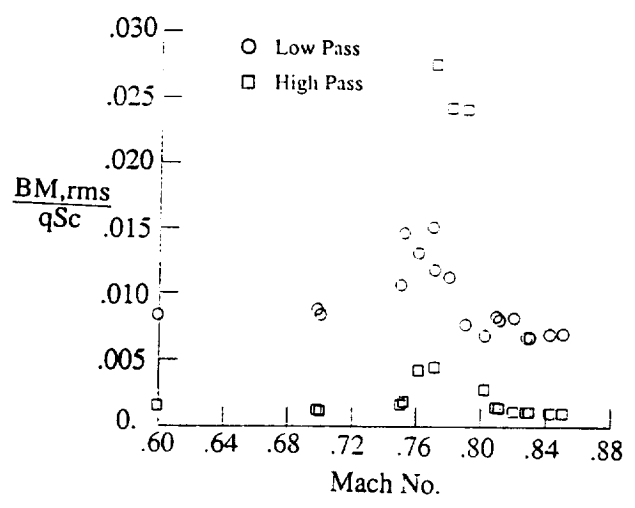


Figure 16. Filtered measured bending moment with vortex generators, configuration 2.

Concluding Remarks

A simple cantilevered flexible wing with an 18% thick circular-arc airfoil was tested in the Langley Transonic Dynamics Tunnel at Mach numbers where transonic shock-boundary layer oscillations occur. Several model configurations and some potential fixes to the oscillations were tested.

In the region of shock-boundary layer oscillations, an increased random buffeting level was found for the first bending mode which was at a much lower frequency than the frequency of the shock-boundary layer oscillations. A limit-cycle oscillation was found for a "third-bending-like" mode which involved splitter plate motion and had a natural frequency which was near the frequency of the shock-boundary layer oscillations.

A large effect of the boundary layer transition strip was found for the relatively low Reynolds number of these tests. Erratic results were obtained for free transition (transition-strip removed).

A small spanwise strip mounted behind the shock wave effectively eliminated the shock-boundary layer oscillations but significantly increased the subsonic buffeting level of the first bending mode. One configuration of wishbone-type vortex generators also reduced the shock-boundary layer oscillations but led to a flutter condition. Another configuration of vortex generators had little effect. The experience with these attempted fixes indicates that fixes derived on rigid models need verification on a dynamic model.

Acknowledgements

We wish to acknowledge the significant assistance of Clifford J. Obara of the Lockheed Engineering and Sciences Company, Hampton, Virginia, with the application of liquid crystals and of John C. Lin of the Low Turbulence Pressure Tunnel Section of NASA Langley Research Center with vortex generator application.

References

- ¹Nixon, D. , ed., Unsteady Transonic Aerodynamics, vol. 120, Progress in Astronautics and Aeronautics, AIAA, Washington, DC, 1989.
- ²McDevitt, J. B.; Levy, L. L., Jr.; and Deiwert, G. S., "Transonic Flow About a Thick Circular-Arc Airfoil," AIAA Journal, vol. 14, May 1976, pp. 606-613.
- ³Finke, K., "Unsteady Shock Wave-Boundary Layer Interaction on Profiles in Transonic Flow," AGARD-CPP-168, May 1975, Paper 28.
- ⁴Seegmiller, H. L.; Marvin, J. G.; and Levy, L. L., Jr., "Steady and Unsteady Transonic Flow," AIAA Paper 78-160, January 1978.
- ⁵Levy, L. L., Jr., "Experimental and Computational Steady and Unsteady Transonic Flows About a Thick Airfoil," AIAA Journal, vol. 16, June 1978, pp. 564-572.
- ⁶McDevitt, J. B., "Supercritical Flow About a Thick Circular-Arc Airfoil," NASA TM-78549, 1979.
- ⁷Mabey, D. G., "Oscillatory Flows from Shock-Induced Separations in Biconvex Airfoils in Ventilated Wind Tunnels," AGARD-CP-296, Paper 11, 1980.
- ⁸Levy, L. L., Jr., "Predicted and Experimental Steady and Unsteady Flows About a Biconvex Airfoil," NASA TM-81262, 1981.
- ⁹Mabey, D. G.; Wlesh, B. L.; and Cripps, B. E., "Periodic Flows on a Rigid 14% Thick Biconvex Wing at Transonic Speeds," Royal Aircraft Establishment, TR-81-059, 1981.
- ¹⁰Gallus, H. E.; Broichhausen, K. D.; and Henne, J. M., "Experimental Unsteady Shock-Boundary Layer Interaction at Single Blades and in Linear Cascades," ASME Paper 86-GT-218, 1986.
- ¹¹Gibb, J., "The Cause and Cure of Periodic Flows at Transonic Speeds," ICAS, 1988, Paper 3.10.1.
- ¹²Yamamoto, K., and Tanida, Y., "Self Excited Oscillation of Transonic Flow Around an Airfoil in Two-Dimensional Channel," ASME Paper 89-GT-58, 1989.
- ¹³Raghunathan, S.; Hall, D. E.; and Mabey, D. G., "Alleviation of Shock Oscillations in Transonic Flow by Passive Controls," Aeronautical Journal, Aug./Sept. 1990, pp. 245-250, AIAA Paper 90-0046.
- ¹⁴Mohan, S. R., "Periodic Flows on Rigid Aerofoils at Transonic Speeds," AIAA Paper 91-0598, January 1991.
- ¹⁵Herzberg, N., "Suppression of Shock Oscillations on a Biconvex Airfoil," MSC Thesis, Cranfield Institute of Technology, 1986.
- ¹⁶McDevitt, J. B.; and Okuno, A. F., "Static and Dynamic Pressure Measurements on NACA 0012 Airfoil in the AMES High Reynolds Number Facility," NASA TP-2485, 1985.
- ¹⁷Hirose, N.; and Miwa, H., "Computational and Experimental Research on Buffet Phenomena of Transonic Airfoils," Japanese NAL TR-996T, 1988.
- ¹⁸Girodroux-Lavigne, P.; and LeBalleur, J. C., "Time Consistent Computation of Transonic Buffet Over Airfoils," ICAS Paper 88-5.5.2, 1988.
- ¹⁹Lee, B. H. K., "Oscillatory Shock Motion Caused by Transonic Shock Boundary-Layer Interaction," AIAA Journal, vol. 28, no. 5, pp. 942-944, May 1990.
- ²⁰Stanewsky, E.; and Basler, D., "Experimental Investigation of Buffet Onset and Penetration on Supercritical Airfoil at Transonic Speeds," Paper No. 4, AGARD CP-483, 1990.
- ²¹Holmes, B. J.; and Obara, C. J., "Advances in Flow Visualization Using Liquid-Crystal Coatings," SAE Paper 871017, 1987.
- ²²Mabey, D. G.; Ashill, P. R.; and Welsh, B. L., "Aeroelastic Oscillations Caused by Transitional Boundary Layers and Their Attenuation," Journal of Aircraft, vol. 24, July 1987, pp. 463-469.

- ²³Hoimes, A. E., Hickey, P. K.; Murphy, W. R.; and Hilton, D. A., "The Application of Sub-Boundary Layer Vortex Generators to Reduce Canopy "Mach Rumble" Interior Noise of the Gulfstream III", AIAA Paper 87-0084, January 1987.
- ²⁴Kehro, M.; Hutchenson, S.; Liebeck, R.; and Blackwelder, R., "Vortex Generators Used to Control Laminar Separation Bubbles," AIAA Paper 90-0051, January 1990.
- ²⁵Lin, J. C.; Howard, F. G.; Bushnell, D. M.; and Selby, G. V., "Investigation of Several Passive and Active Methods for Turbulent Flow Separation Control," AIAA Paper 90-1598, June 1990.
- ²⁶Moss, G. F.; and Pierce, D., "The Dynamic Response of Wings in Torsion at High Subsonic Speeds" AGARD CP-226, Paper 4, April 1977.



Report Documentation Page

1. Report No. NASA TM 104088		2. Government Accession No.		3. Recipient's Catalog No.	
4. Title and Subtitle Transonic Shock-Induced Dynamics of a Flexible Wing With a Thick Circular-Arc Airfoil			5. Report Date May 1991		
			6. Performing Organization Code		
7. Author(s) R. M. Bennett, B. E. Dansberry, M. G. Farmer, C. V. Eckstrom, D. A. Seidel, and J. A. Rivera, Jr.			8. Performing Organization Report No.		
			10. Work Unit No. 509-10-02-03		
9. Performing Organization Name and Address NASA Langley Research Center Hampton, Virginia 23665-5225			11. Contract or Grant No.		
			13. Type of Report and Period Covered Technical Memorandum		
12. Sponsoring Agency Name and Address National Aeronautics and Space Administration Washington, DC 20546-0001			14. Sponsoring Agency Code		
			15. Supplementary Notes Presented as AIAA Paper No. 91-1107 at the 32nd Structures, Structural Dynamics and Materials Conference, Baltimore, Maryland, April 7-10, 1991.		
16. Abstract Transonic shock-boundary layer oscillations occur on rigid models over a small range of Mach numbers on thick circular-arc airfoils. Extensive tests and analyses of this phenomena have been made in the past but essentially all of them were for rigid models. A simple flexible wing model with an 18% circular arc airfoil was constructed and tested in the Langley Transonic Dynamics Tunnel to investigate the dynamic characteristics that a wing might have under these conditions. In the region of shock-boundary layer oscillations, buffeting of the first bending mode was obtained. This mode was well separated in frequency from the shock boundary layer oscillations. A limit cycle oscillation was also measured in a "third-bending-like" mode, involving wing vertical bending and splitter plate motion, which was in the frequency range of the shock-boundary layer oscillations. Several model configurations were tested, and a few potential fixes were investigated.					
17. Key Words (Suggested by Author(s)) Unsteady Transonic Aerodynamics Aeroelasticity and Flutter Shock-Boundary Layer Interaction			18. Distribution Statement Unclassified - Unlimited Subject Category 02		
19. Security Classif. (of this report) Unclassified		20. Security Classif. (of this page) Unclassified		21. No. of pages 11	22. Price A03

